

Enhancing vapor generation at a liquid-solid interface using micro/nanoscale surface structures fabricated by femtosecond laser surface processing

Troy P. Anderson, Chris Wilson, Craig A. Zuhlke, Corey Kruse, George Gogos, Sidy Ndao, and Dennis Alexander

Troy P. Anderson^{*a}, Chris Wilson^a, Craig A. Zuhlke^a, Corey Kruse^b, George Gogos^b, Sidy Ndao^b,
Dennis Alexander^a

Department of Electrical Engineering, University of Nebraska - Lincoln, 209N Scott Engineering Center, Lincoln, NE, USA 68588, Department of Mechanical & Materials Engineering, University of Nebraska - Lincoln, W342 Nebraska Hall, Lincoln, NE, USA 68588

ABSTRACT

Femtosecond Laser Surface Processing (FLSP) is a versatile technique for the fabrication of a wide variety of micro/nanostructured surfaces with tailored physical and chemical properties. Through control over processing conditions such as laser fluence, incident pulse count, polarization, and incident angle, the size and density of both micrometer and nanometer-scale surface features can be tailored. Furthermore, the composition and pressure of the environment both during and after laser processing have a substantial impact on the final surface chemistry of the target material. FLSP is therefore a powerful tool for optimizing interfacial phenomena such as wetting, wicking, and phase-transitions associated with a vapor/liquid/solid interface. In the present study, we utilize a series of multiscale FLSP-generated surfaces to improve the efficiency of vapor generation on a structured surface. Specifically, we demonstrate that FLSP of stainless steel 316 electrode surfaces in an alkaline electrolysis cell results in increased efficiency of the water-splitting reaction used to generate hydrogen. The electrodes are fabricated to be superhydrophilic (the contact angle of a water droplet on the surface is less than 5 degrees). The overpotential of the hydrogen evolution reaction (HER) is measured using a 3-electrode configuration with a structured electrode as the working electrode. The enhancement is attributed to several factors including increased surface area, increased wettability, and the impact of micro/nanostructures on the bubble formation and release. Special emphasis is placed on identifying and isolating the relative impacts of the various contributions.

Keywords: Femtosecond Laser Surface Processing, Electrolysis, Vapor Generation, Overvoltage

1. INTRODUCTION

Femtosecond Laser Surface Processing (FLSP) is a power fabrication technique that enables the tuning of the physical, optical, electrical, and thermal properties of a metal surface through the generation of a rich variety of microscale and nanoscale surface features directly out of the substrate material. The exceptional durability of metallic surface structures fabricated using FLSP techniques make them attractive for tailoring the multiphase interactions with an adjacent liquid/vapor such as generating extraordinary shifts in the Leidenfrost point of a material in film boiling^{1,2}, increasing the heat transfer coefficient of nucleate boiling³, and the generation of hydrogen gas via electrolysis⁴. In the current paper, the various impacts of FLSP-generated surface structures on the efficiency of the hydrogen evolution reaction (HER) in an alkaline electrolysis cell are characterized. Alkaline electrolysis represents one of the most scalable and environmentally sustainable methods for generating hydrogen gas to be used as an alternative energy source and also serves as an ideal platform for the study of the impact of FLSP-generated surface features on interfacial energy transfer.

In an electrolysis cell, hydrogen gas is generated by driving a current between two electrodes immersed in an electrolytic aqueous solution and the production rate is directly related to the electrochemical current by Faraday's law. The efficiency of an electrolysis cell is a function of the voltage required to drive a given current. While the thermoneutral voltage that defines a 100% efficient electrolysis cell is 1.48 V (i.e. all of the input electrical energy is transferred to

generating vapor rather than heat), practical electrolysis cells operate at a higher voltage due to losses within the system. The excess voltage above the thermoneutral voltage is called the overvoltage. The losses that contribute to the overvoltage of the cell can be depicted as resistances and are summarized in the following equation:

$$R_{total} = R_1 + R_{electrodes} + R_{bubble} + R_{electrolyte} + R_{ions} + R_2$$

, where R_{total} is the total resistance of the reaction, R_1 is the electrical resistance of the connections from the voltage source to the anode, $R_{electrodes}$ is the resistance of the ionic reaction at the electrodes, R_{bubble} is the resistance from the bubbles covering the electrode surface, $R_{electrolyte}$ is the electrical resistance of the electrolyte in the electrochemical system, R_{ions} is the resistance from the transfer of ions in the bulk electrolyte to the electrode, and R_2 is the resistance of the connects from the voltage source to the cathode⁵.

Various approaches to increasing electrolysis efficiency by targeting $R_{electrodes}$ and R_{bubble} have been explored including material or surface geometry modifications of the electrodes⁶⁻¹¹. The goal of this approach is to improve the efficiency of the electrode/electrolyte interface by tailoring the electrode surface for better performance, e.g. less interfacial resistance, larger surface area, enhanced nucleation sites, etc. For example, several groups have applied transition metal alloys to standard electrode materials in an attempt to improve electrochemical activity¹¹⁻¹⁵. However, drawbacks of these approaches include poor stability¹⁵ or high cost. Surface structures have also been shown to impact the electrolysis efficiency both experimentally and theoretically^{13,16-18}. It was found that by varying the height or the porosity of the 3D structures, the kinetics of the reaction could be modified. In the present work, Linear Scanning Voltammetry (LSV) is used on a series of stainless steel electrode surfaces in order to isolate and measure the various mechanisms by which FLSP-generated surface structures impact electrolysis efficiency. The surface structures are similar in topology to the Gaussian structures theoretically simulated by Compton et al.¹⁸, which can be used to influence surface area and wettability. It is expected that this will reduce the overvoltage of the electrochemical system. The effects of the modified electrode surface area and wettability due to FLSP are explored to determine the impact that each component has on the electrolysis of water.

2. EXPERIMENT

The purpose of this study is to characterize the mechanisms by which FLSP improves the efficiency of a stainless steel electrode in an alkaline electrolysis cell. A specific emphasis is placed on the effects of the surface structure on the generation of a vapor bubble as opposed to a modification of the electrochemistry. This distinction enables the results of this paper to be applied to any electrochemical system.

In order to determine the effect of physical surface shaping on the electrolysis efficiency, a series of six samples was fabricated that included five structured samples and one unstructured sample as a control. Femtosecond Laser Surface Processing (FLSP) was used to fabricate multiscale hierarchal surface structures on electrode surfaces. All of the structured surfaces are characterized by a quasi-periodic pattern of conical mound structures covered by a layer of nanoparticles. The structures generated during the FLSP processing step are a result of reshaping the substrate material via a combination of growth mechanisms including preferential ablation, capillary flow of laser-induced melt layers, and redeposition of ablated surface features. In the range of laser parameters considered in this study, the surfaces morphologies span from below surface growth mounds (BSG-mounds) to above surface growth mounds (ASG-mounds)¹⁹⁻²¹.

2.1 Experimental Setup

The laser used was a Ti:Sapphire laser (Spitfire, Spectra Physics) capable of producing 1 mJ, 50 fs pulses with a center wavelength of 800 nm at a repetition rate of 1 kHz. The pulse length of the laser was monitored and optimized using a Frequency Resolved Optical Gating (FROG) instrument from Positive Light (Model 8-02). The schematic of the experimental setup has been previously published^{4,19,20}. To generate laser-processed surface features, a target electrode was placed on a 3D computer-controlled translation stage and translated through a laser beam with a Gaussian profile. The laser illumination was performed in ambient atmosphere.

After FLSP processing, high-resolution images of the surfaces were taken using a scanning electron microscope (SEM) and surface profiles were taken using a Keyence VK-X200 laser confocal scanning microscope. The Keyence system has an axial resolution of 0.5 nm and a transverse resolution of 120 nm. The structure spacing was determined by performing a 2D Fast Fourier Transform (FFT) on the SEM images and determining the peak spatial frequency. The structure size was measured by generating a binary image from the SEM image after smoothing via morphological

image processing. The surface area ratio and the average peak to valley height were taken from the Keyence 3D surface profiles.

The surface morphologies chosen for the electrochemical experiments were chosen based off of a larger grid of surface structures created on 316 SS by varying laser fluence and incident pulse count using the laser setups described in Sections. The specific surfaces were chosen based off of increasing structure spacing as laser fluence increased and increase structure size as the laser pulse count increased. The grid of surfaces created along with the selected surface is shown in Figure 1. A table with the relevant physical characteristics is shown in Table 1.

Table 1: Data corresponding to FLSP electrodes derived from SEM images and 3D confocal microscope laser scans

Laser Fabrication Parameters		Physical Characteristics			
Peak Fluence (J/cm ²)	Shot Number	Average Peak to Valley Height (μm)	Surface Area Ratio	Structure Spacing (px)	Structure Size (px)
3.12	300	36.8	4.9	8.2	5.7
3.12	400	41.8	5.4	12.3	6.1
3.12	500	41.0	3.8	14.8	7.0
3.12	600	44.4	5.2	13.4	6.2
3.12	700	43.4	5.2	16.4	5.5
3.12	800	45.7	5.2	14.8	5.9

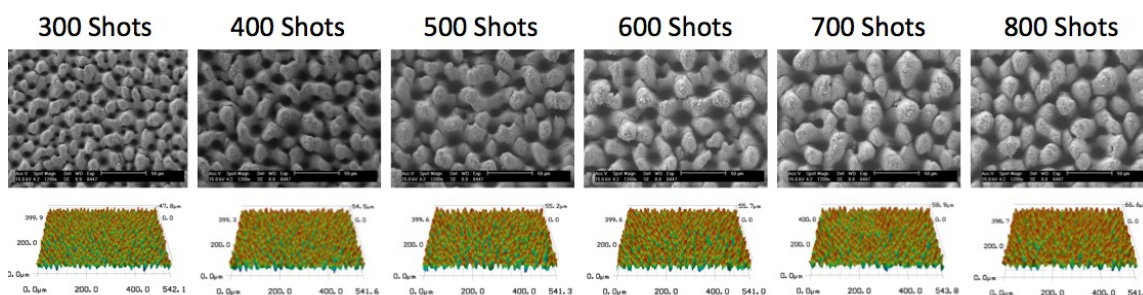


Figure 1: Scanning electron microscope images (left) and 3D optical surface profiles (right) of stainless steel 316 surfaces.

2.2 Electrochemical Analysis

A custom electrochemical cell was used for the work presented. An isometric rendering of the cell can be found in Figure 2. The acrylic cell shown in Figure 2 was designed to constrict movement of the electrodes. Acrylic was chosen as the material for the cell as acrylic is resistant to basic solutions. The electrodes were positioned so that the center lines of the electrodes are lined up in each experiment. The cell was also designed to hold 175 mL of solution. The purpose of this specific solution volume was to keep only the FLSP portion of the working electrode in the electrolyte. The separation distance between the working and counter electrode surfaces was 22 mm.

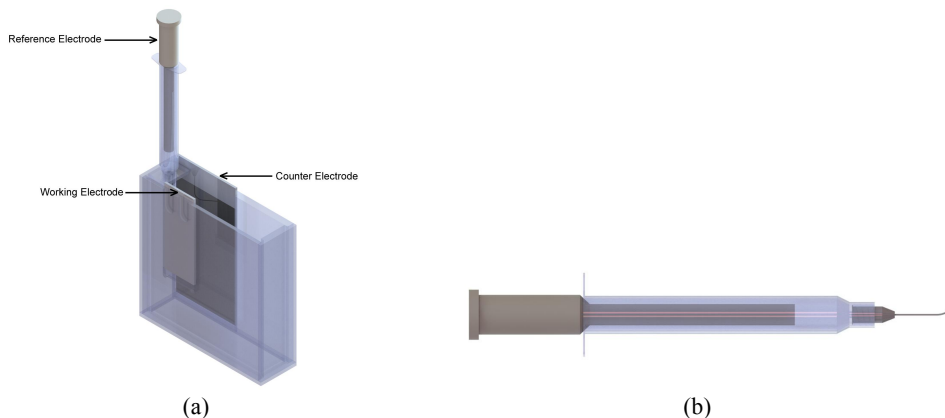


Figure 2: (a) Schematic of custom three electrode cell used for LSV experiments. (b) Schematic of Luggin-Haber capillary

The reference electrode was a CH Instruments 152 Alkaline/Mercury Oxide reference electrode with a standard voltage of 0.098 V versus a normal hydrogen electrode (NHE). The reference electrode is housed in a syringe body filled with the electrolyte and a bent needle tip is attached at the end of the body. The syringe body, along with the needle tip, acts as a Luggin-Haber capillary. The purpose of a Luggin-Haber capillary is to reduce ohmic overpotential, which is proportional to the distance between the working electrode surface and the reference electrode tip²². The tip was placed ~2 mm of the surface as any distance closer to the surface did not yield an appreciable difference in results.

The electrolyte was 3M KOH(aq) created using 85% KOH(s) pellets from Sigma-Aldrich mixed with distilled water. 175 mL of the electrolyte was used to ensure that only the FLSP portion of the electrode participated in the reaction. A 99.999% nitrogen gas flow of 60 SCCM over the cell was in place for the duration of all experiments. The purpose of this flow was to shield the electrolyte from the ambient air since KOH(aq) absorbs carbon dioxide and water vapor. An additional flow of nitrogen gas was bubbled through the cell to degas the solution of oxygen before each LSV measurement. Each LSV dataset represents an average of nine LSV scans with the error bars representing the standard deviation of the data.

3. RESULTS AND DISCUSSION

Linear Scanning Voltammetry plots of the hydrogen evolution reaction (HER) on the electrode surfaces are shown in Figure 3 with the electrochemical current as a function of the applied voltage with respect to the reference electrode in Figure 3(a) and a magnified portion of Figure 3(a) that more clearly shows the difference in performance between the processed and polished electrodes given in Figure 3(b). The processed electrodes outperform the polished electrode in all cases; a smaller absolute voltage relative to the reference electrode is required to produce a given electrochemical current. Specifically, the overvoltage reduction ranges from 164 to 192 mV across the series of FLSP-processed electrodes. There is a slight trend indicating that an increase in surface structure height and the associated increase in surface area ratio lead to an increase of efficiency, which is seen as a shift of the LSV curves to the right (less absolute voltage required to achieve a given current).

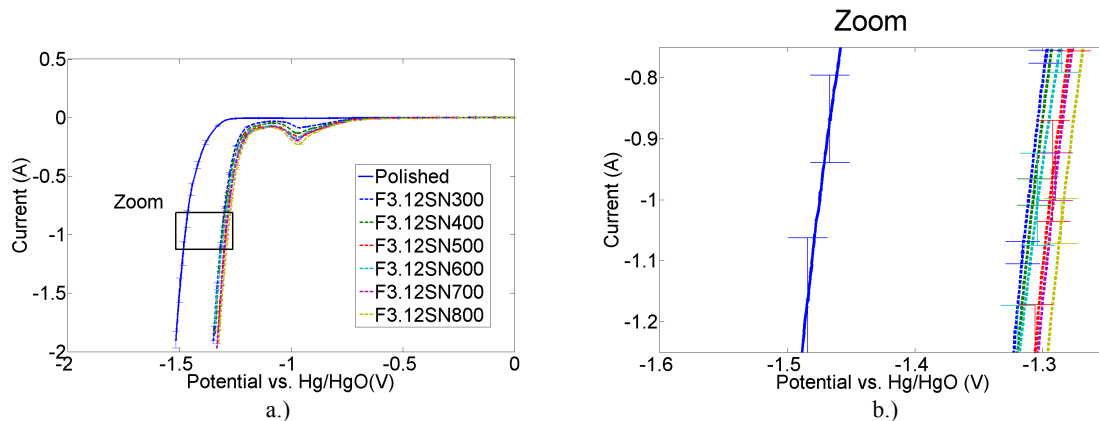


Figure 3: (a) Linear scanning voltammetry analysis of the electrochemical current associated with the hydrogen evolution reaction with respect to the applied voltage. (b) A magnified view of the boxed region within (a)

Since the output current is directly related to the electrode surface area through Faraday's law, a plot of the current density with respect to applied voltage (see Figure 4) provides insight into the effect of the FLSP-generated surface structures independent of the surface area that they provide. The current density with respect to the applied voltage is shown in Figure 4(a); a magnified region highlighting the performance of the electrodes for a current density in the range of 15 to 25 A/cm² is given in Figure 4(b). The surface area used to calculate the current density was measured using the Keyence optical profiler. Similar to Figure 3, a subtle trend can be seen in that increasing the structure height increases performance, even beyond the error bars. More important, however, is that observation that all of the processed electrodes outperform the polished electrode, with a reduction of overvoltage ranging from 69 to 100 mV. The increase in surface area of FLSP-structured electrodes only accounts for 49%-58% of the reduction of overvoltage. The remaining reduction in overvoltage gained through the FLSP process is due to additional phenomena.

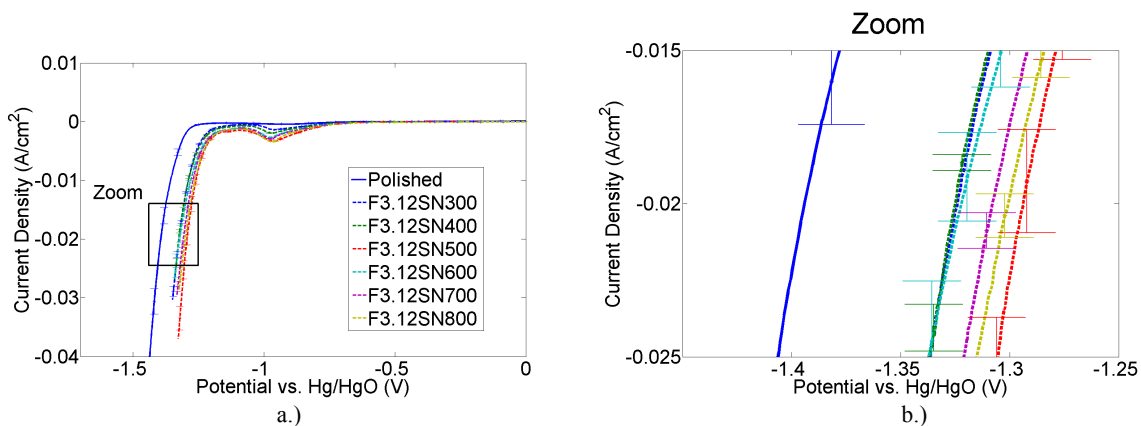


Figure 4: (a) Linear scanning voltammetry analysis of the electrochemical current density associated with the hydrogen evolution reaction with respect to the applied voltage. (b) A magnified view of the boxed region within (a)

In addition to modifying the surface area, the surface structures generated through the FLSP process increase the electrolysis efficiency by modifying the formation and release of bubbles from the surface (ref last years paper). This can occur both through a modification of the wettability or by physically limiting the size of the bubbles by the surface structure geometry²³⁻²⁵. To determine the impact of wettability on the electrolysis efficiency, the performance of the polished surfaces before and after cleaning in both pure oxygen and ambient air were compared to the FLSP-structured surfaces. The impact of plasma cleaning is to remove organic or carbon surface layers from the electrodes. The FLSP electrodes were all superhydrophilic with contact angles less than 5° whereas the polished electrode has a contact angle of about 35° before plasma cleaning. The air plasma processing was conducted for 10 minutes and produced a surface with an average contact angle of 12.1°. The oxygen plasma cleaning was conducted for 30 minutes and produced a surface with an average contact angle of 9.8°. The resulting LSV curves are shown in Figure 5. Note that only the

FLSP-processed electrode surface fabricated with 400 pulses per spot is included in the plot for clarity. This sample represents the FLSP electrode with the smallest reduction in overvoltage. This sample was chosen to be a conservative representation of the impact of FLSP.

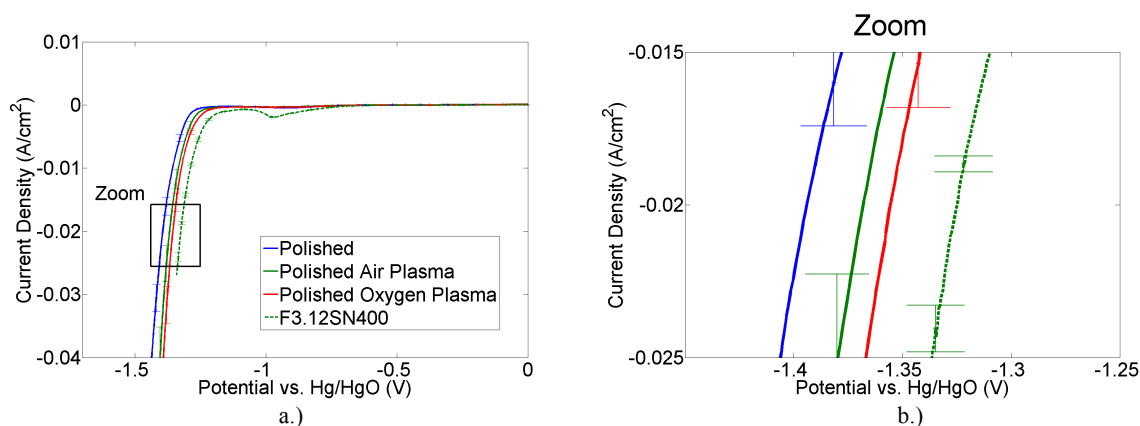


Figure 5: (a) Linear scanning voltammetry analysis of the electrochemical current density associated with the hydrogen evolution reaction with respect to the applied voltage highlighting the impact of modifying the wettability of polished electrodes via plasma cleaning. (b) A magnified view of the boxed region within (a)

From Figure 5, it can be seen that the decrease of the contact angle after plasma cleaning both in ambient air and pure oxygen improves the performance (by shifting the LSV curve to the right). It should be noted that the plasma cleaning process performed in air or pure oxygen has no measurable impact on the wettability of the FLSP-processed surfaces. This may be due to the extremely low contact of the surfaces prior to cleaning. The overvoltage reduction between the best performing polished sample and the worst performing FLSP sample is 30 mV. It is expected that the wettability as measured by the contact angle would not completely account for the remaining efficiency enhancement associated with the FLSP structured surfaces. The remainder of the overvoltage reduction is attributed to the ability of the geometry of the microscale surface structures to control the growth and release of the bubbles. This is further evidenced by the subtle trend that correlates increasing structure height with increased performance.

4. CONCLUSION

The various mechanisms by which the fabrication of surface structures on stainless steel electrodes using Femtosecond Laser Surface Processing (FLSP) techniques have been characterized in an alkaline electrolysis cell. FLSP-structured electrodes increase performance by increasing the surface area, modifying the surface wettability, and physically controlling the growth of vapor bubbles. The maximum reduction in overvoltage achieved to generate a current of 1 A was 192 mV. Of this, 49% of the reduction was attributed to the surface area increase. The separate effects of wettability and physical surface shaping are closely linked. However, plasma cleaning to modify the wettability of polished surfaces reveals that at least 36% of the overvoltage reduction associated with FLSP-structured surfaces can be attributed to the wettability as measured by the static contact angle. The remaining overvoltage reduction is attributed to physical surface shaping.

ACKNOWLEDGMENTS

This work has been supported by a NASA EPSCoR Grant # NNX13AB17A, a NASA Space Grant # NNX10AN62H and a grant through the Nebraska Center for Energy Sciences Research (NCESR) with funds provided by Nebraska Public Power District (NPPD) to the University of Nebraska-Lincoln (UNL) # 4200000844.

5. REFERENCES

- [1] Kruse, C., Anderson, T. P., Wilson, C., Zuhlke, C., Alexander, D. R., Gogos, G., Ndao, S., "Extraordinary Shifts of the Leidenfrost Temperature from Multiscale Micro/Nanostructured Surfaces," *Langmuir* **29**(31), 9798–9806 (2013).
- [2] Hassebrook, A., Kruse, C., Wilson, C., Anderson, T., Zuhlke, C., Alexander, D., Gogos, G., Ndao, S., "Effects of droplet diameter on the Leidenfrost temperature of laser processed multiscale structured surfaces," *Fourteenth Intersoc. Conf. Therm. Thermomechanical Phenom. Electron. Syst.*, 452–457 (2014).
- [3] Kruse, C. M., Anderson, T., Wilson, C., Zuhlke, C., Alexander, D., Gogos, G., Ndao, S., "Enhanced pool-boiling heat transfer and critical heat flux on femtosecond laser processed stainless steel surfaces," *Int. J. Heat Mass Transf.* **82**, 109–116 (2015).
- [4] Anderson, T. P., Wilson, C., Zuhlke, C. A., Kruse, C., Hassebrook, A., Somanas, I., Ndao, S., Gogos, G., Alexander, D., "Tailoring liquid/solid interfacial energy transfer: fabrication and application of multiscale metallic surfaces with engineered heat transfer and electrolysis properties via femtosecond laser surface processing techniques," *Proc. SPIE 8968, Laser-based Micro- Nanoprocessing VIII*, 89680R (March 6, 2014) (2014).
- [5] Zeng, K., Zhang, D., "Recent progress in alkaline water electrolysis for hydrogen production and applications," *Prog. Energy Combust. Sci.* **36**(3), 307–326, Elsevier Ltd (2010).
- [6] Bamwenda, G. R., Tsubota, S., Nakamura, T., Haruta, M., "Photoassisted hydrogen production from a water-ethanol solution: a comparison of activities of Au-TiO₂ and Pt-TiO₂," *J. Photochem. Photobiol. A Chem.* **89**(2), 177–189 (1995).
- [7] Moir, J., Soheilnia, N., O'Brien, P., Jelle, A., Grozea, C. M., Faulkner, D., Helander, M. G., Ozin, G. a., "Enhanced hematite water electrolysis using a 3D antimony-doped tin oxide electrode.," *ACS Nano* **7**(5), 4261–4274 (2013).
- [8] Ni, M., Leung, M. K. H., Leung, D. Y. C., Sumathy, K., "A review and recent developments in photocatalytic water-splitting using TiO₂ for hydrogen production," *Renew. Sustain. Energy Rev.* **11**(3), 401–425 (2007).
- [9] El-Deab, M. S., Ohsaka, T., "Manganese oxide nanoparticles electrodeposited on platinum are superior to platinum for oxygen reduction.," *Angew. Chem. Int. Ed. Engl.* **45**(36), 5963–5966 (2006).
- [10] Feng, L., Vrubel, H., Bensimon, M., Hu, X., "Easily-prepared dinickel phosphide (Ni₂P) nanoparticles as an efficient and robust electrocatalyst for hydrogen evolution.," *Phys. Chem. Chem. Phys.* **16**(13), 5917–5921 (2014).
- [11] Morales-Guio, C. G., Tilley, S. D., Vrubel, H., Grätzel, M., Hu, X., "Hydrogen evolution from a copper(I) oxide photocathode coated with an amorphous molybdenum sulphide catalyst.," *Nat. Commun.* **5**(1), 3059 (2014).
- [12] Jaramillo, T., Jørgensen, K., Bonde, J., "Identification of active edge sites for electrochemical H₂ evolution from MoS₂ nanocatalysts," *Science* **317**(5834), 100–102 (2007).
- [13] Huang, Y.-J., Lai, C.-H., Wu, P.-W., Chen, L.-Y., "Ni Inverse Opals for Water Electrolysis in an Alkaline Electrolyte," *J. Electrochem. Soc.* **157**(3), 18–22 (2010).
- [14] Ben Aoun, S., Dursun, Z., Sotomura, T., Taniguchi, I., "Effect of metal ad-layers on Au(111) electrodes on electrocatalytic reduction of oxygen in an alkaline solution," *Electrochem. commun.* **6**(8), 747–752 (2004).
- [15] Fan, C., Piron, D., Slebo, A., Paradis, P., "Study of Electrodeposited Nickel-Molybdenum, Nickel-Tungsten, Cobalt-Molybdenum, and Cobalt-Tungsten as Hydrogen Electrodes in Alkaline Water Electrolysis," *J. Electrochem. Soc.* **141**(2), 382–387 (1994).
- [16] Kim, S., Koratkar, N., Karabacak, T., Lu, T.-M., "Water electrolysis activated by Ru nanorod array electrodes," *Appl. Phys. Lett.* **88**(26), 263106 (2006).
- [17] Menshkykau, D., Compton, R. G., "The Influence of Electrode Porosity on Diffusional Cyclic Voltammetry," *Electroanalysis* **20**(22), 2387–2394 (2008).
- [18] Menshkykau, D., Streeter, I., Compton, R. G., "Influence of Electrode Roughness on Cyclic Voltammetry," *J. Phys. Chem. C* **112**(37), 14428–14438 (2008).
- [19] Zuhlke, C. A., Anderson, T. P., Alexander, D. R., "Formation of multiscale surface structures on nickel via above surface growth and below surface growth mechanisms using femtosecond laser pulses," *Opt. Express* **21**(7), 8460–8473 (2013).
- [20] Zuhlke, C. A., Anderson, T. P., Alexander, D. R., "Fundamentals of layered nanoparticle covered pyramidal structures formed on nickel during femtosecond laser surface interactions," *Appl. Surf. Sci.* **21**(7), 8460–8473 (2013).
- [21] Zuhlke, C. A., Anderson, T. P., Alexander, D. R., "Comparison of the structural and chemical composition of two unique micro/nanostructures produced by femtosecond laser interactions on nickel," *Appl. Phys. Lett.* **103**(12), 121603 (2013).

- [22] Bard, A., Faulkner, L., *Electrochemical Methods: Fundamentals and Applications*, 2nd ed., 27, Wiley, New Delhi (2006).
- [23] Vogt, H., Balzer, R. J., "The bubble coverage of gas-evolving electrodes in stagnant electrolytes," *Electrochim. Acta* **50**(10), 2073–2079 (2005).
- [24] Vogt, H., "The actual current density of gas-evolving electrodes—Notes on the bubble coverage," *Electrochim. Acta* **78**, 183–187 (2012).
- [25] Wüthrich, R., Comminellis, C., Bleuler, H., "Bubble evolution on vertical electrodes under extreme current densities," *Electrochim. Acta* **50**(25-26), 5242–5246 (2005).